

Monte Carlo simulation of terahertz harmonic generation in GaAs quantum wire structure

Andrei V. Borzdov, Vladimir M. Borzdov, Vladimir A. Labunov

Abstract—Electron transport in the GaAs/AlAs quantum wire transistor structure is simulated by means of ensemble Monte Carlo method under the effect of external alternating electric field. Nonlinear properties of electron transport are studied in terahertz range. The efficiency of high order harmonics generation in the structure is estimated for the lattice temperature of 300 K.

Keywords—Electron transport, GaAs quantum wire, Monte Carlo simulation, terahertz generation.

I. INTRODUCTION

ELECTRICAL properties of semiconductor structures with one-dimensional electron gas have been intensively investigated for decades. A³B⁵ quantum wires have been considered as the basis of novel high electron mobility transistors operating at very high frequencies. State-of-the-art technologies allow fabrication of field-effect transistors based on thin quantum wires with gate-all-around structures [1], [2]. Such quantum wire transistors could be promising for the use as elements of modern integrated circuits.

By now electrical characteristics of semiconductor quantum wire structures, including quantum wire based field-effect transistors, have been studied by means of different approaches [3]–[6], as well as by Monte Carlo method [7], [8]. Ensemble Monte Carlo simulation has proved its efficiency in simulation of semiconductor structures and devices. One of the advantages of the method is the possibility of inclusion into the simulation complex physical effects such as rigorous description of scattering processes, quantum effects, realistic description of the band structure and other.

Modern integrated circuits tend to operate at rather high frequencies, so transient and periodic processes occurring in the circuit elements are of great interest too. Transient and periodic processes in the systems with one-dimensional electron gas can be also investigated with the help of ensemble Monte Carlo simulations [9], [10].

As a result of miniaturization process, the elements of integrated circuits are forced to operate under the effect of alternating electric fields with rather high strengths. The

charge carrier transport under such conditions exhibit strongly nonlinear properties. In connection with this, the possibility to use the nonlinear transport properties for generation of radiation in terahertz range has attracted much attention recently. The method to ascertain the efficiency of high order harmonic generation was proposed in [11], [12], and the generation efficiency was calculated for bulk semiconductors. Also the efficiency was calculated for submicron diodes [13]. The possibility to use quantum wire structure as an ultra high frequency generator was proposed in [14]. In the latter work ballistic electron transport was considered.

The aim of our study is to investigate the possibility and ascertain the efficiency of high order harmonics generation in the GaAs quantum wire structure in the range of fundamental frequencies from 0.2 THz to 1 THz. In our study we investigate electron transport in the approximation of infinitely long quantum wire, so that electron transport in the structure is controlled by electron scattering in the wire channel. In that case the nonlinearity of electron transport occurs due to scattering processes and intersubband transitions.

II. CALCULATION OF ELECTRON STATES IN THE WIRE

In present study electron transport is simulated in gate-all-around GaAs/AlAs quantum wire transistor structure. The schematic cross-section of the wire is represented in Fig. 1. The structure consists of a thin 10 nm×10 nm GaAs channel surrounded by AlAs barrier layer. The thickness of AlAs is supposed to be 5 nm. The gate is aluminum.

Electron transport in the structure occurs due to the application of external electric field along the Z-direction. In the given structure electron motion is free along the wire channel (Z-direction) and is spatially confined in transverse dimensions X and Y. The latter leads to electron energy quantization and formation of so called one-dimensional

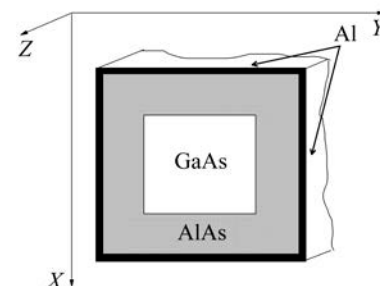


Fig. 1 the schematic cross-section of the simulated quantum wire

Andrei V. Borzdov is with Belarusian State University, Minsk, 220030 Belarus (e-mail: borzdovav@bsu.by).

Vladimir M. Borzdov is with Belarusian State University, Minsk, 220030 Belarus (corresponding author e-mail: borzdov@bsu.by).

Vladimir A. Labunov is with Belarusian State University of Informatics and Radioelectronics, Minsk, 220013 Belarus (e-mail: labunov@bsuir.by).

energy subbands. To define subband energies and electron wave functions the numerical solution of corresponding Schrodinger and Poisson equations must be performed.

The Schrodinger equation for the wire in parabolic band approximation takes the following form [15], [16]

$$-\frac{\hbar^2}{2} \nabla \cdot \left(\frac{1}{m^*(x, y)} \nabla \psi_i(x, y) \right) + V(x, y) \psi_i(x, y) = E_i \psi_i(x, y), \quad (1)$$

where \hbar is the Planck constant, $m^*(x, y)$ is the position dependent electron effective mass, $\psi_i(x, y)$ is the electron wave function in i -th subband, and E_i is the subband energy. $V(x, y)$ is the potential energy given by the equation

$$V(x, y) = V_h(x, y) + V_{xc}(x, y) - e\phi(x, y), \quad (2)$$

where $V_h(x, y)$ is the potential describing the conduction band offset between GaAs and AlAs, $V_{xc}(x, y)$ is the exchange-correlation potential, e is the magnitude of electron charge and $\phi(x, y)$ is the electrostatic potential. The electrostatic potential in the structure is derived via the solution of the Poisson equation

$$\nabla \cdot (\varepsilon_0 \varepsilon(x, y) \nabla \phi(x, y)) = en_e(x, y) \quad (3)$$

with ε_0 being the electric constant and $\varepsilon(x, y)$ – the position dependent relative permittivity of the material. Electron concentration $n_e(x, y)$ is defined by the formula [15]

$$n_e(x, y) = \sum_i |\psi_i(x, y)|^2 \int_{E_i}^{\infty} \frac{\sqrt{2m^*(x, y)}}{\pi \hbar \sqrt{E - E_i}} \frac{dE}{1 + \exp((E - E_f)/k_B T)}, \quad (4)$$

where E_f is the Fermi energy, k_B is the Boltzmann constant and T is the lattice temperature. The system of equations (1)–(4) is solved self-consistently.

For the solution of the Schrodinger equation the extraction-orthogonalization procedure described in [16] is used. In present simulation model we consider electron transport only in Γ valley of GaAs. The treatment of the free electron motion along the wire channel takes into account the nonparabolicity of the dispersion relation. The Poisson equation is solved by means of successive overrelaxation method. The boundary condition for electron wave function implies that it vanishes at the semiconductor-metal interface. Boundary condition for the Poisson equation is defined by the applied gate bias. It is assumed that the position of the Fermi level and, as a result, the electron concentration in the structure is controlled by the gate bias. The Schottky barrier height for Al/AlAs system is as high as 1.15 eV [17].

III. ELECTRON SCATTERING RATES CALCULATION

Electron scattering rates are calculated with account of collisional broadening. The calculation procedure includes electron scattering by confined modes of acoustic and polar optical phonons, and GaAs/AlAs interface roughness scattering.

Acoustic phonon scattering is treated in elastic approximation. The corresponding overall scattering rate for electron transitions from initial subband i to all the final subbands j is given by the formula [18]–[20]

$$\begin{aligned} [W_{f,b}]_i^A(E, \eta_i) &= \frac{B_{ac}^2 k_B T \sqrt{2m^*(x, y)}}{2\hbar^2 v^2 \rho} \\ &\cdot \sum_j D_{ij}(E, \Delta E_{ij}, \eta_i) \iint |\psi_i(x, y)|^2 |\psi_j(x, y)|^2 dx dy \end{aligned} \quad (5)$$

with

$$D_{ij}(E, \Delta E_{ij}, \eta_i) = \Theta(E - \Delta E_{ij}) \sqrt{\frac{\eta_i + \sqrt{(E - \Delta E_{ij})^2 + \eta_i^2}}{(E - \Delta E_{ij})^2 + \eta_i^2}}.$$

In the equations above E is the electron kinetic energy, ρ is the density of GaAs, v is the sound velocity in GaAs, B_{ac} is the acoustic deformation potential, η_i is the collisional broadening term, $\Delta E_{ij} = E_j - E_i$, and Θ is the unit step function. Subscripts “f” and “b” stand for “forward” and “backward” scattering processes, respectively. In the case of (5) the rates of forward and backward scattering processes are equal.

Polar optical phonon scattering rate is defined as follows [18]–[20]

$$\begin{aligned} [W_{f,b}^{e/a}]_i^{PO}(E, \eta_i) &= \sum_{\alpha} \frac{e^2 \omega_{\alpha} \sqrt{2m_{\alpha}^*}}{\hbar L_x L_y} \left(\frac{1}{\varepsilon_{\alpha}^{\infty}} - \frac{1}{\varepsilon_{\alpha}} \right) \left(n_{\alpha} + \frac{1}{2} \pm \frac{1}{2} \right) \\ &\cdot \sum_j D_{ij}(E, \Delta E_{ij} \pm \hbar \omega_{\alpha}, \eta_i) \\ &\cdot \sum_{p=1}^{\infty} \sum_{r=1}^{\infty} \frac{|M_{pr}^{ij}|^2}{[q_{f,b}^{e/a}]_{\alpha}^2 + (p\pi/L_x)^2 + (r\pi/L_y)^2} \end{aligned} \quad (6)$$

with

$$\begin{aligned} M_{pr}^{ij} &= \int_0^{L_x} \int_0^{L_y} S_{\alpha}(x, y) \psi_i^*(x, y) \psi_j(x, y) \\ &\cdot \sin(p\pi x/L_x) \sin(r\pi y/L_y) dx dy, \end{aligned}$$

$$[q_f^{e/a}]_\alpha = \frac{\sqrt{2m_\alpha^* E}}{\hbar} - \frac{\sqrt{2m_\alpha^* (E - \Delta E_{ij} \mp \hbar \omega_\alpha)}}{\hbar},$$

$$[q_b^{e/a}]_\alpha = \frac{\sqrt{2m_\alpha^* E}}{\hbar} + \frac{\sqrt{2m_\alpha^* (E - \Delta E_{ij} \mp \hbar \omega_\alpha)}}{\hbar},$$

where ω_α is the phonon frequency, $\varepsilon_\alpha^\infty$ и ε_α are the optic and static permittivities of the material, respectively, n_α is the Bose-Einstein distribution function. Subscript α stands for material, i.e. $\alpha = \text{GaAs}$ or AlAs , and superscripts “e/a” stand for processes with phonon emission and absorption, respectively. L_x and L_y are the transverse dimensions of the structure. $S_\alpha(x, y)$ is the step function which satisfies the following conditions: S_{GaAs} is equal to 1 in GaAs and is equal to 0 in AlAs, and S_{AlAs} is equal to 1 in AlAs and is equal to 0 in GaAs. In “ \pm ” and “ \mp ” the upper sign corresponds to the process with phonon emission and the lower one to the process with phonon absorption, respectively.

Finally, the surface roughness scattering in the wire must be considered due to the imperfectness of the GaAs/AlAs interface. Taking into account that there are two by two scattering planes in the wire (denoted by subscripts 1 and 2 for partial derivatives in each direction) and basing on the results of [20], [21], we arrive at the following expression for the surface roughness scattering rate

$$[W_{\text{rb}}]_i^{\text{SR}}(E, \eta_i) =$$

$$= \frac{1}{4} \left[\left[\left(\frac{\partial E_i}{\partial L_x} \right)_1^2 + \left(\frac{\partial E_i}{\partial L_x} \right)_2^2 \right] \frac{1}{1 + \Lambda^{-1} L_y (a + b(1 + 4\pi \Lambda L_y^{-1})^{-1})} \right.$$

$$+ \left. \left[\left(\frac{\partial E_i}{\partial L_y} \right)_1^2 + \left(\frac{\partial E_i}{\partial L_y} \right)_2^2 \right] \frac{1}{1 + \Lambda^{-1} L_x (a + b(1 + 4\pi \Lambda L_x^{-1})^{-1})} \right]$$

$$\cdot \frac{\sqrt{\pi} \Lambda^2 \Lambda \sqrt{2m^*}}{2\hbar^2} \frac{\sqrt{D(E, \Delta E_{ij} = 0, \eta_i)}}{1 + \pi \Lambda^2 K(E)^2 ((E \mp E + \eta_i)/2)}. \quad (7)$$

In (7) $K(E) = \sqrt{2m^* E} / \hbar$, Δ is the surface roughness amplitude and Λ is the roughness correlation length. Parameters Δ and Λ are supposed equal for all scattering planes. For certainty the values of the surface roughness amplitude and correlation length are the following: $\Delta = 0.5$ nm and $\Lambda = 6$ nm. The values of the parameters $a = 0.163438$ and $b = 0.105886$ were obtained in [21]. Current model implies that the surface roughness scattering is elastic and intrasubband process.

IV. MONTE CARLO SIMULATION RESULTS AND DISCUSSION

In our simulations we suppose that the external alternating electric field is varying in time according to harmonic law of the following form

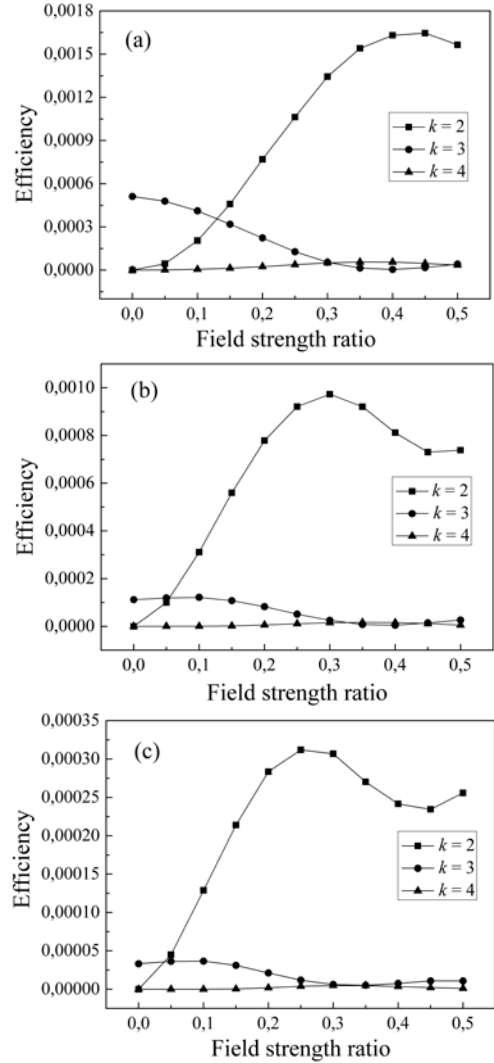


Fig. 2 the efficiency of high order harmonics generation: (a) $-f = 0.2$ THz, (b) $-f = 0.5$ THz, (c) $-f = 1$ THz

$$F(t) = F_0 + F_m \sin(2\pi ft), \quad (8)$$

where F is the field strength, F_0 is the strength of the constant field component, F_m is the amplitude of alternating field component, f is the frequency, and t is time. In our previous works [9], [10], [20] we restricted our simulations to the case of electric quantum limit, i.e. population of the only one lowest subband was taken into account. The approximation of electric quantum limit is appropriate for thin quantum wires and moderate electric field strengths. To make the results of our current calculations adequate for regarded field strengths we took into account up to 8 electron energy subbands while solving the Schrodinger equation. The lattice temperature was taken 300 K.

The Monte Carlo simulation starts with initial Maxwell distribution of electron momentum in the direction of free motion. At the beginning of the simulation electrons populate the lowest energy subband. Simulation continues for a period of time which is enough for the cyclostationary conditions to be established. Simulation data are collected after this period

of time.

For a given electron density in the structure, electric current in the channel is defined by electron drift velocity. In this case the efficiency of the k th harmonic generation can be expressed as the ratio of its intensity I_k to the intensity of the fundamental one I_1 according to the following formula [11]

$$I_k/I_1 = a_k^2 / (k^2 a_1^2), \quad (9)$$

where a_k are coefficients of the Fourier transform of the electron drift velocity versus time dependence, which is obtained from the Monte Carlo simulation.

In the Fig. 2 the efficiency defined by (9) is plotted versus the field strength ratio F_0/F_m (see formula (8)). The value of F_m is 10^5 V/m. The gate voltage is 0 V. The efficiency was calculated for the external field frequency range from 0.2 THz to 1 THz with the step 0.1 THz. In the figure the results for $f = 0.2$ THz, $f = 0.5$ THz and $f = 1$ THz are presented. The results are plotted only for three higher harmonics as the efficiency of other harmonics ($k > 4$) is too low for the considered electric field strength values. When the constant field component is zero, only odd harmonics are present. As it can be seen from the figure, the efficiency of the second and the fourth harmonic generation increases with the growth of F_0 . At the same time the efficiency of the third harmonic decreases. In the examined range of F_0/F_m ratio a local maximum of the second harmonic generation efficiency is observed for the ratio in the interval from 0.25 to 0.45.

The results of calculations show that the efficiency of high order harmonics generation in the quantum wire structure under considered conditions is lower in comparison with bulk GaAs and submicron diode structures [11], [13]. This may be caused by the fact that the amplitude of the electric field strength regarded in our work is lower than that used for bulk materials. We restricted our calculations to the case of $F_m = 10^5$ V/m and $F_0 = 5 \cdot 10^4$ V/m as electron transport is simulated only in Γ valley of GaAs. At higher field strengths electron transitions to L and X valleys must be sufficient which may lead to higher nonlinearity of electron transport and, in turn, to higher generation efficiency.

V. CONCLUSION

In present study the nonlinearity of electron transport in GaAs quantum wire structure has been investigated and the possibility of high order harmonics generation has been shown. Though the calculated generation efficiency under considered conditions may be lower for the quantum wire structure than for bulk materials, quantum wire structures must be superior in electronics applications due to lower parasitic capacities.

In our work we considered an approximation of "infinitely" long quantum wire. So the investigation of harmonics generation in quantum wire structures with finite channel lengths, particularly in quantum wire field-effect transistors, must be an interesting point.

REFERENCES

- [1] S. Sasaki, K. Tateno, G. Zhang, H. Suominen, Y. Harada, S. Saito, A. Fujiwara, T. Sogawa, K. Muraki, "Encapsulated gate-all-around InAs nanowire field-effect transistors," *Appl. Phys. Lett.*, vol. 103, pp. 213502-1–213502-5, 2013.
- [2] C. Zhang, W. Choi, P. K. Mohseni, X. Li, "InAs planar nanowire gate-all-around MOSFETs on GaAs substrates by selective lateral epitaxy," *IEEE Electron Device Lett.*, vol. 36, no. 7, pp. 663–665, 2015.
- [3] D. Jovanovic, J.-P. Leburton, "Quantum confinement and charge control in deep mesa etched quantum wire devices," *IEEE Electron Device Lett.*, vol. 14, no. 1, pp. 7–9, 1993.
- [4] S. K. Islam, F. C. Jain, "Analysis of quantum wire high electron mobility transistor," *Solid-State Electron.*, vol. 39, no. 4, pp. 615–620, 1996.
- [5] M. Abul Khayer, R. K. Lake, "Modeling and performance analysis of GaN nanowire field-effect transistors and band-to-band tunneling field-effect transistors," *J. Appl. Phys.*, vol. 108, pp. 104503-1–104503-7, 2010.
- [6] V. Gupta, R. S. Gupta, R. Kumar Singh, "A comparative study of Si, Ge and GaAs cylindrical nanowire transistors with non equilibrium Greens function approach," *J. Comput. Theor. Nanosci.*, vol. 11, no. 5, pp. 1330–1334, 2014.
- [7] S. Briggs, J.-P. Leburton, "Size effects in multisubband quantum wire structures," *Phys. Rev. B*, vol. 38, no. 12, pp. 8163–8170, 1988.
- [8] K. Hess (editor), *Monte Carlo device simulation: full band and beyond*, Boston/Dordrecht/London: Kluwer Academic Publishers, 1991, ch. 7.
- [9] D. Pozdnyakov, A. Borzdov, V. Borzdov, F. Komarov, "Modelling of non-stationary electron transport in semiconductor nanowires and carbon nanotubes," *Proc. SPIE*, vol. 7025, pp. 70251S-1–70251S-9, 2008.
- [10] D. Pozdnyakov, A. Borzdov, V. Borzdov, V. Labunov, "Calculation of electrophysical parameters of thin undoped GaAs-in- Al_2O_3 quantum nanowires and single-wall armchair carbon nanotubes," *Proc. SPIE*, vol. 7521, pp. 75210S-1–75210S-9, 2010.
- [11] D. Persano Adorno, M. Zarccone, G. Ferrante, "Far-infrared harmonic generation in semiconductors: a Monte Carlo simulation," *Laser Physics*, vol. 10, no. 1, pp. 310–315, 2000.
- [12] D. Persano Adorno, M. Zarccone, G. Ferrante, "Monte Carlo simulation of harmonic generation in InP," *Laser and Particle Beams*, vol. 19, pp. 81–84, 2001.
- [13] D. Persano Adorno, M. C. Capizzo, M. Zarccone, "Monte Carlo simulation of harmonic generation in GaAs structures operating under large-signal conditions," *J. Comput. Electron.*, no. 6, pp. 26–30, 2007.
- [14] L. Fedichkin, V. V'yurkov, "Quantum ballistic channel as an ultrahigh frequency generator," *Appl. Phys. Lett.*, vol. 64, pp. 2535–2536, 1994.
- [15] G. L. Snider, I.-H. Tan, E. L. Hu, "Electron states in mesa-etched one-dimensional quantum well wires," *J. Appl. Phys.*, vol. 68, no. 6, pp. 2849–2853, 1990.
- [16] D. Jovanovic, J.-P. Leburton, "Self-consistent analysis of single-electron charging effects in quantum-dot nanostructures," *Phys. Rev. B*, vol. 49, no. 11, pp. 7474–7483, 1994.
- [17] C. Berthod, N. Binggeli, A. Baldereschi, "Schottky barrier heights at polar metal/semiconductor interfaces," *Phys. Rev. B*, vol. 68, no. 8, pp. 085323-1–085323-11, 2003.
- [18] A. V. Borzdov, D. V. Pozdnyakov, V. O. Galenchik, V. M. Borzdov, F. Komarov, "Self-consistent calculations of phonon scattering rates in the GaAs transistor structure with one-dimensional electron gas," *phys. stat. sol. (b)*, vol. 242, no. 15, pp. R134–R136, 2005.
- [19] A. V. Borzdov, D. V. Pozdnyakov, "Scattering of electrons in the GaAs/AIAs transistor structure," *Phys. Solid State*, vol. 49, no. 5, pp. 963–967, 2007.
- [20] A. V. Borzdov, D. V. Pozdnyakov, V. M. Borzdov, A. A. Orlikovsky, V. V. V'yurkov, "Effect of a transverse applied electric field on electron drift velocity in a GaAs quantum wire: a Monte Carlo simulation," *Rus. Microelectronics*, vol. 39, no. 6, pp. 411–417, 2010.
- [21] D. Pozdnyakov, "Influence of surface roughness scattering on electron low-field mobility in thin undoped GaAs-in- Al_2O_3 nanowires with rectangular cross-section," *phys. stat. sol. (b)*, vol. 247, no. 1, pp. 134–139, 2010 (see also corrections to the paper, *phys. stat. sol. (b)*, vol. 247, no. 5, pp. 1248, 2010).